JOURNAL OF GEOPHYSICAL RESEARCH, VOL. 102, NO. A2, PAGES 2165-2173, FEBRUARY 1, 1997

Study of the solar wind deceleration upstream of the Martian terminator bow shock

G. Kotova,[1] M. Verigin,[1] A. Remizov,[1] N. Shutte,[1] H. Rosenbauer,[2] S. Livi,[2] K. Szegö,[3] M. Tatrallyay,[3] J. Slavin,[4] J. Lemaire,[5] K. Schwingenschuh,[6] and T.-L. Zhang[6]

Abstract. Solar wind plasma and magnetic data obtained near the Martian terminator bow shock by the TAUS energy spectrometer and the MAGMA magnetometer onboard the Phobos 2 spacecraft are analyzed. It is revealed that on average the solar wind stream is slowing down just upstream of the bow shock. Nearly inverse correlation is found between the values of the velocity decrease and the undisturbed solar wind density for the outbound (mostly quasi-parallel) bow shock crossings, while for the inbound crossings (mostly quasi-perpendicular) this correlation is observed only for the velocity decrease upstream of the shock foot. This result permits us to distinguish between the two possible reasons causing solar wind deceleration: (1) mass loading of the solar wind flow by planetary ions originating from the corona of Mars, and (2) solar wind protons reflected from the bow shock. The solar wind deceleration upstream of the bow shock foot turned to be approximately dawn-dusk symmetric. On the basis of the revealed relation between the velocity decrease and upstream solar wind density, a coronal density profile is deduced which is in agreement with earlier results for the subsolar region. According to this profile, the density of the hot oxygen corona of Mars might be ~ 3 times higher in the period of observations than the estimations of the "extreme" corona model suggests, even taking into account the possible contribution of the hydrogen corona to the solar wind deceleration effect.

Introduction

The solar wind deceleration upstream of the Martian bow shock was immediately recorded when the Phobos 2 spacecraft became the orbiter of Mars. *Verigin et al.* [1991] analyzed the observations of the TAUS instrument in the first three elliptical orbits around Mars and found a solar wind deceleration of about 100 km s^{-1} upstream of the subsolar bow shock. It was emphasized that this deceleration can be caused by the mass loading of the plasma flow by ions originating from the hot oxygen-hydrogen corona of Mars and/or by protons reflected from the bow shock. Taking into account only the mass loading effect by oxygen ions, the upper limit of the density distribution of the planetary oxygen corona and the upper limit of the loss rate of oxygen from the atmosphere through the corona were evaluated. However, the solar wind deceleration of about 100 km s^{-1} implies that the hot oxygen corona of Mars could be 5 times denser than was anticipated by the model of *Ip* [1988, 1990], which estimated the highest density compared to other models.

The preshock deceleration of the solar wind in the third elliptical orbit was also analyzed in the paper by *Barabash and Lundin* [1993] on the basis of the ASPERA instrument data. According to the their estimates, about 60% of the observed solar wind velocity decrease was attributed to the specularly reflected ions. *Dubinin et al.*, [1994] studied the first four elliptical orbits and found an asymmetry in the preshock solar wind density increase, probably an effect of the changing orientation of the interplanetary magnetic field.

According to theoretical [*Goodrich*, 1985; *Wilkinson and Schwartz*, 1990; *Onsager and Thomsen* 1991, and references therein] and experimental [*Sckopke et al.*, 1983; *Gosling and Robson*, 1985] studies of the terrestrial bow shock, up to 20-30% of incoming solar wind protons [*Sckopke et al.*, 1983] can be specularly reflected at a quasi-perpendicular shock. These ions are then turned around by the magnetic field and returned back to the shock, providing a deceleration of the solar wind on a short scale length of $\leq r_{g\perp} = V_\perp/\omega_{gi}$, where $V_\perp$ is the solar wind velocity component normal to the bow shock front and ω_{gi} is the proton gyrofrequency [*Neugebauer*, 1970; *Sckopke et al.*, 1983]. In the case of quasi-parallel shocks, specularly reflected protons have guiding center motions directed away from the shock, and they are really recorded upstream of the bow shock, but according to the observations [*Gosling et al*, 1982], they constitute only ~ 3 % of the incident solar wind density.

The deceleration of the solar wind is commonly observed in the Earth's foreshock region [*Bame et al.*, 1980; *Bonifazi et al.*, 1980]. This deceleration is caused by the so-called "diffuse" ions backstreaming from the bow shock. These ions should exist upstream of the Martian quasi-parallel bow shock too and affect the solar wind stream.

This study will try to separate different factors causing the solar wind deceleration upstream of the Martian bow shock,

[1] Space Research Institute, Russian Academy of Sciences, Moscow, Russia.
[2] Max-Planck-Institut für Aeronomie, Katlenburg-Lindau, Germany.
[3] KFKI Research Institute for Particle and Nuclear Physics, Budapest, Hungary.
[4] NASA Goddard Space Flight Center, Greenbelt, Maryland.
[5] Belgisch Instituut voor Ruimte-Aeronomie, Brussels, Belgium.
[6] Space Research Institute, Graz, Austria.

Paper number 96JA01533.
0148-0227/97/96JA-01533$09.00

taking into account the different characteristics of ion reflection at quasi-parallel and quasi-perpendicular shocks. The expected inverse dependence of the coronal mass loading deceleration on the solar wind density [*Verigin et al.*, 1991] will be examined for the evaluation of the role of the oxygen-hydrogen corona in the solar wind deceleration upstream of the Martian bow shock. Upstream solar wind parameters observed by the Phobos 2 TAUS instrument for 70 bow shock crossings will be presented and studied statistically together with magnetic field measurements performed by the MAGMA instrument in order to update estimations of the properties of the hot oxygen-hydrogen corona of Mars.

Instrumentation and Data Description

The TAUS instrument is an energy spectrometer designed for the investigation of the solar wind interaction with Mars [*Rosenbauer et al.*, 1989a]. It could measure proton, alpha-particle, and heavy ion ($M/q > 3$) spectra separately in the energy per charge range of 30 V to 6 kV subdivided into 32 energy channels. The instrument had a field of view of ~ 40° × 40° centered on the nominal aberrated solar wind direction and divided into 8 × 8 angular channels. A complete proton spectrum was measured within 8 s. The MAGMA magnetometer measured one magnetic field vector in every 1.5 or 45 s, depending on the telemetry mode in the range ±100 nT with a resolution of 0.05 nT [*Aydogar et al.*, 1989].

In the present study, data measured in the circular orbits of Phobos 2 (~ 9500 km from the center of the planet) quasi-synchronous with the orbit of the Phobos moon are considered. For this time interval (February 20 to March 26, 1989), one proton spectrum in the energy range 150 - 6000 eV per 2 min and one magnetic field vector per 45 s were obtained. Most of the time the Phobos 2 spacecraft lost three-axis stabilization. The angle between its rotation axis and the Sun-Mars line was sometimes approaching 20°. Therefore only the magnitude of the magnetic field vector is used for the analysis. The Martian bow shock crossings were identified by the sudden decrease of the mean energy and broadening in the proton spectra and by the simultaneous increase of the magnetic field magnitude [*Rosenbauer et al.*, 1989b].

TAUS plasma data from 41 inbound and 29 outbound legs of the circular orbits are used to study the solar wind deceleration upstream of the Martian terminator bow shock. (Few orbits were excluded from the analysis because of essential velocity jumps close to the bow shock in the upstream region.) Magnetic field data were available for 36 inbound and 26 outbound bow shock passes of the above cases.

Observations

Figure 1 presents an overview of solar wind velocity profiles measured during 1 hour upstream of the Martian terminator bow shock for all selected inbound and outbound legs of the Phobos 2 circular orbits. The velocity values V estimated from measured proton spectra are shown relative to the solar wind reference velocity V_r marked by the horizontal lines. V_r was obtained by averaging over an ~ 20-min window ~50 min upstream of the

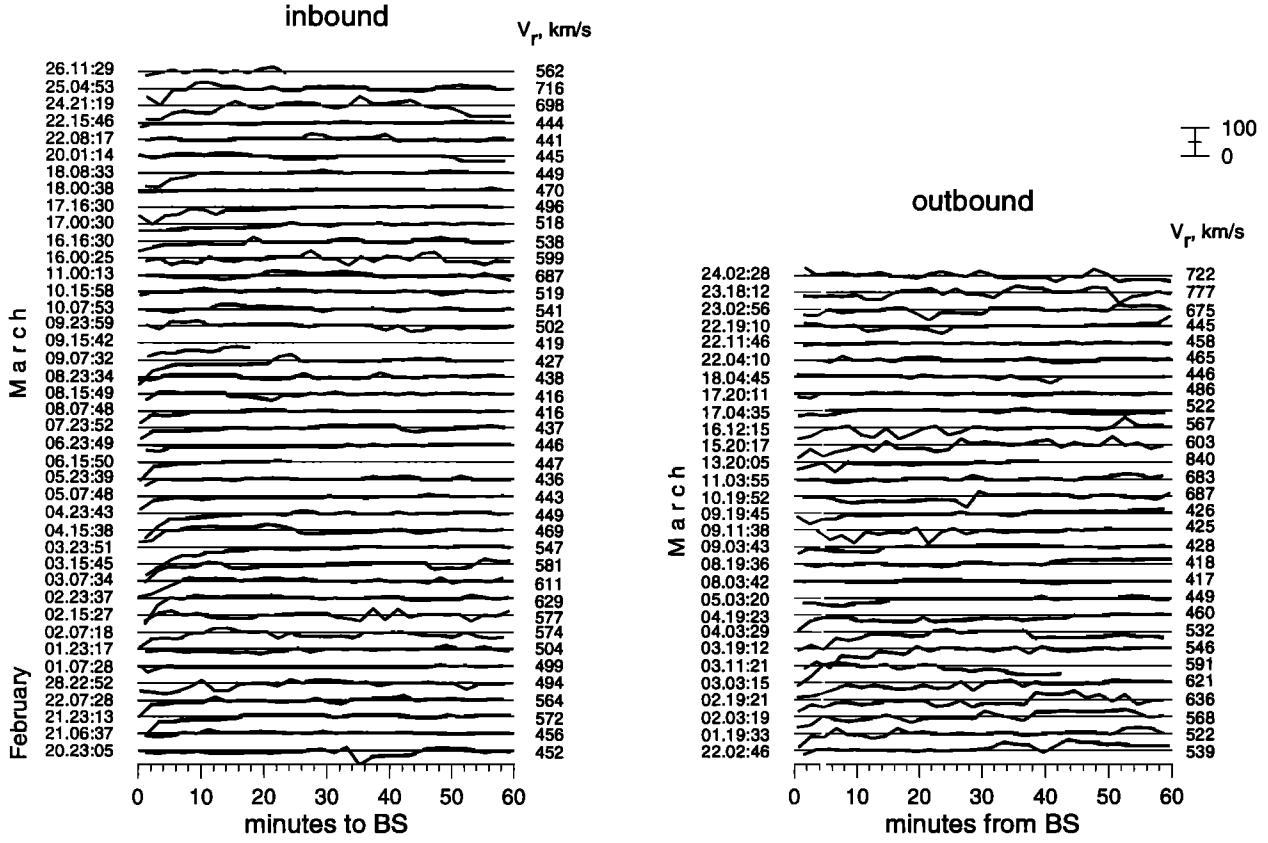

Figure 1. Solar wind velocity profiles measured upstream of the Martian terminator bow shock for inbound and outbound legs of the Phobos 2 circular orbits. The times of bow shock crossings and the upstream reference velocities are indicated.

bow shock crossing. The position of the window was taken closer to the bow shock when plasma discontinuities were observed. The dates and times of bow shock crossings (t=0) are shown on the left of the profiles; in case of multiple crossings the outermost location was considered. Figure 1 demonstrates that the solar wind deceleration just upstream of the bow shock is a common feature of both sets of data, but not all crossings show the slowing of the solar wind upstream of the bow shock. There are a number of reasons which can obscure solar wind deceleration, for example, natural velocity variations of the solar wind, outward motion of the bow shock, dependence of the deceleration effect on the solar wind density, etc.

The average angle of ~56° between the spiral interplanetary magnetic field and the Sun-Mars line suggests that quasi-perpendicular shocks can be expected more frequently in inbound legs while quasi-parallel shocks are more typical in outbound legs. The rotation of the spacecraft makes impossible to distinguish reliably quasi-perpendicular and quasi-parallel bow shock crossings for most of the circular orbits, though some conclusions could be drawn on the basis of variations of the magnetic field magnitude across the bow shock and the ratio of magnetic field magnitudes measured in the magnetosheath and in the undisturbed solar wind.

Figure 2 presents examples of the solar wind parameter variations upstream of an inbound and an outbound bow shock crossing. In both cases the spacecraft was rotating, but the axis of rotation (and consequently the axis of the TAUS field of view) looked roughly toward the Sun, as the regular density fluctuations were relatively small according to TAUS data. On March 2 at 2337 UT, Phobos 2 crossed a quasi-perpendicular bow shock as it is seen from the profile of the magnetic field magnitude across the shock with the overshoot and foot regions. Using bow shock models [*Slavin et al.*, 1991; *Zhang et al.*, 1991] and despun magnetic field components, the angle ϑ_{BN} between the upstream magnetic field direction and the shock normal was determined as $\vartheta_{BN} \approx 67°$. On March 2, 0319 UT, the spacecraft crossed a quasi-parallel bow shock with the estimated angle $\vartheta_{BN} \approx 40°$. In the inbound case a strong and abrupt deceleration of the solar wind is seen just upstream of the bow shock crossing, while in the outbound case the deceleration is rather gradual.

To illustrate this difference between outbound and inbound bow shock crossings apparently reflecting the difference between quasi-parallel and quasi-perpendicular bow shock crossings, the average relative velocity, density, and temperature profiles are shown in Figure 3 (N_r and T_r are reference density and temperature, respectively, averaged over the same time windows as V_r). Figure 3a presents the above parameters averaged for all the inbound (open circles) and outbound (solid circles) crossings shown in Figure 1. The relative solar wind velocity decrease is about 7% of the reference solar wind velocity upstream of the inbound (dusk side) bow shock crossings and ~4% upstream of the outbound (dawn side) crossings, the deceleration being more abrupt on the dusk side. Rather sharp velocity decrease in the "inbound" profile is likely to be caused by reflected protons in the foot of the bow shock. On the contrary, a more gradual velocity decrease toward the bow shock in the "outbound" profile is probably connected with mass loading of the solar wind by oxygen and hydrogen ions. In the inbound case the mass loading effect is accompanied by the more pronounced

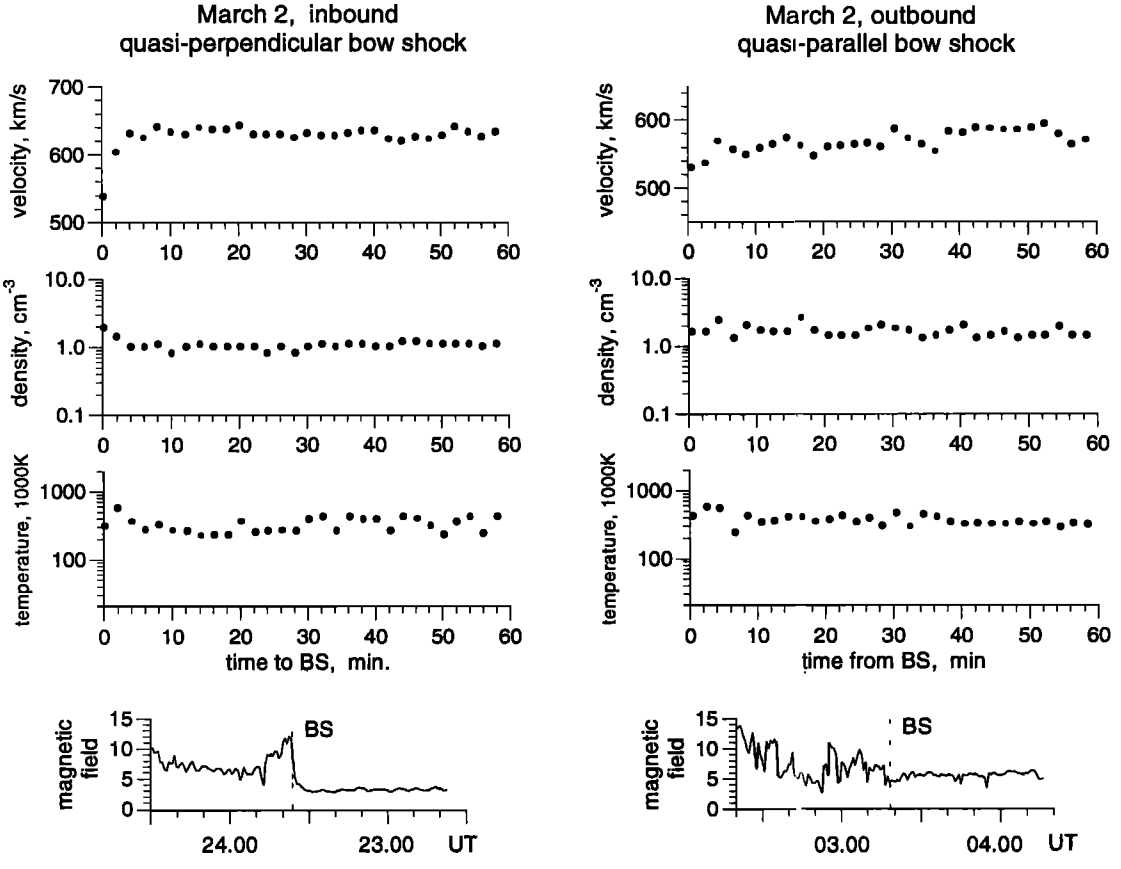

Figure 2. Solar wind parameter variations upstream of an individual inbound and outbound bow shock crossing. Magnetic field profiles are shown across the shocks.

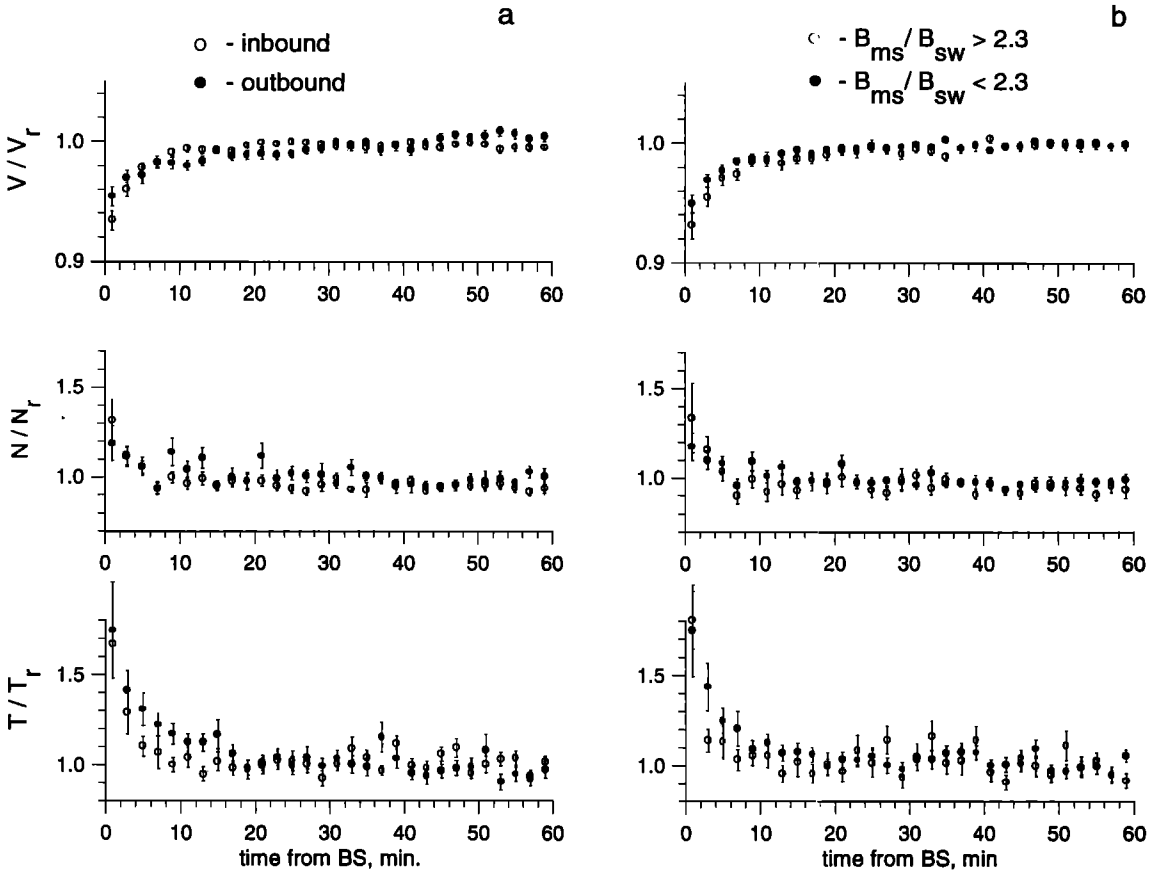

Figure 3. Relative velocity, density and temperature profiles averaged for the bow shock crossings shown in Figure 1. Bars show standard deviations of the points.

effect of specularly reflected protons. In Figure 3b, similar average profiles are calculated on the basis of the value of B_{ms}/B_{sw}, where B_{sw} is the magnitude of the reference upstream solar wind magnetic field and B_{ms} is the magnitude of the magnetosheath magnetic field downstream of the overshoot. Open circles show data obtained in those circular orbits where the magnetic field jump across the bow shock was higher than 2.3 and solid circles present the data when $B_{ms}/B_{sw} < 2.3$. Such a separation can also characterize the difference between quasi-perpendicular and quasi-parallel bow shock crossings (e.g., see Figures 9 and 10 in a comprehensive paper by *Tatrallyay et al.* [1984], taking into account that the magnetosonic Mach number was higher than 3 in almost all Martian bow shock crossings). In Figure 3b the behavior of averaged normalized parameters of the solar wind upstream of the Martian bow shock is more or less the same as in Figure 3a. The difference between the two density profiles both in Figure 3a and in Figure 3b is qualitatively in agreement with the asymmetry in the subsolar observations discussed by *Dubinin et al.* [1994]. The relatively higher temperature observed farther upstream of the bow shock crossings which are supposed to be quasi-parallel is probably due to the broader foreshock region with high wave activity in this case.

It is reasonable to correlate the value of the solar wind velocity decrease with the solar wind density to search whether the solar wind deceleration upstream of a quasi-parallel shock (outbound legs, $B_{ms}/B_{sw} < 2.3$) is mostly caused by the mass loading ions.

Indeed, the equations describing the solar wind mass loading process are given in the paper by *Verigin et al.* [1991, equations (2), (3)]. It was shown that for weakly loaded highly supersonic solar wind as a linear approximation, the solar wind velocity $V(r,\varphi)$ and density $N(r,\varphi)$ (r is the areocentric distance, φ is the angular distance of the point of observation from the subsolar point) variations upstream of the bow shock are described by the equations

$$V(r,\varphi) = V_{sw} - \frac{n_o M_i r_o}{N_{sw}\tau_i} f\left(r,\varphi,\frac{n_1}{n_o},\gamma\right)$$
$$N(r,\varphi) = N_{sw} + \frac{n_o M_i r_o}{V_{sw}\tau_i} g\left(r,\varphi,\frac{n_1}{n_o},\gamma\right), \quad (1)$$

where V_{sw} and N_{sw} are the velocity and density, respectively, of the undisturbed solar wind stream, M_i is the mass of loading ions, τ_i is the ionization time, γ is the ratio of specific heats, n_o and n_1 are the parameters of the model density profile in the corona, described by *Verigin et al.* [1991, equation (1)]:

$$n(r) = n_o\left(\frac{r_o}{r}\right)^2 + n_1\left(\frac{r_o}{r}\right)^5, \quad (2)$$

where the total density of the corona is (n_o+n_1) at $r_o = 10^4$ km. (In the paper by *Verigin et al.* [1991] there were misprints in equation (3b): $(\gamma+1)$ in the second term on the right should be replaced by $(\gamma-1)$ and the coefficient 4 before the term $(\cos^3\varphi - 3\cos\varphi+2)$ should be replaced by 2.) For all the circular orbits of Phobos 2, values of $f(r, \varphi, n_1/n_o, \gamma)$ are almost the same, because all the orbits are similar, and the value of n_1/n_o is determined by the model of the Martian corona. Thus it may be expected that the value of the velocity decrease V_{sw}-V_s (V_s is the

solar wind velocity just upstream of the bow shock) is nearly inversely proportional to the density of the undisturbed solar wind.

In Figure 4, values of the measured velocity decrease V_r-V_s (>5 km s^{-1}) are plotted versus solar wind density N_r for the outbound and inbound crossings of the bow shock and separately for the crossings with the ratio $B_{ms}/B_{sw} < 2.3$ and $B_{ms}/B_{sw} > 2.3$. For the outbound crossings the correlation is reasonably good (the correlation coefficient is $c = 0.54$), while for the inbound crossings the correlation is rather poor ($c = 0.31$). Similarly, the velocity decrease is roughly inversely proportional to the solar wind density upstream of the bow shock with small magnetic field jump (quasi-parallel). This fact suggests that the hot oxygen and/or hydrogen corona of Mars can be considered as the cause of the deceleration of the solar wind upstream of the Martian quasi-parallel (dawn) bow shock. Upstream of the quasi-perpendicular (dusk) bow shock the effect of the Martian corona is obscured by the more pronounced effect of specularly reflected protons.

For quantitative estimations a more accurate approach was used, taking into account the individual bow shock crossing coordinates, the differences between the measured reference parameters V_r and N_r, and the undisturbed solar wind parameters V_{sw} and N_{sw}:

$$V_s = V_{sw} - \frac{n_o M_i r_o}{N_{sw}\tau_i} f_s,$$
$$V_r = V_{sw} - \frac{n_o M_i r_o}{N_{sw}\tau_i} f_r, \qquad (3)$$
$$N_r = N_{sw} + \frac{n_o M_i r_o}{V_{sw}\tau_i} g_r,$$

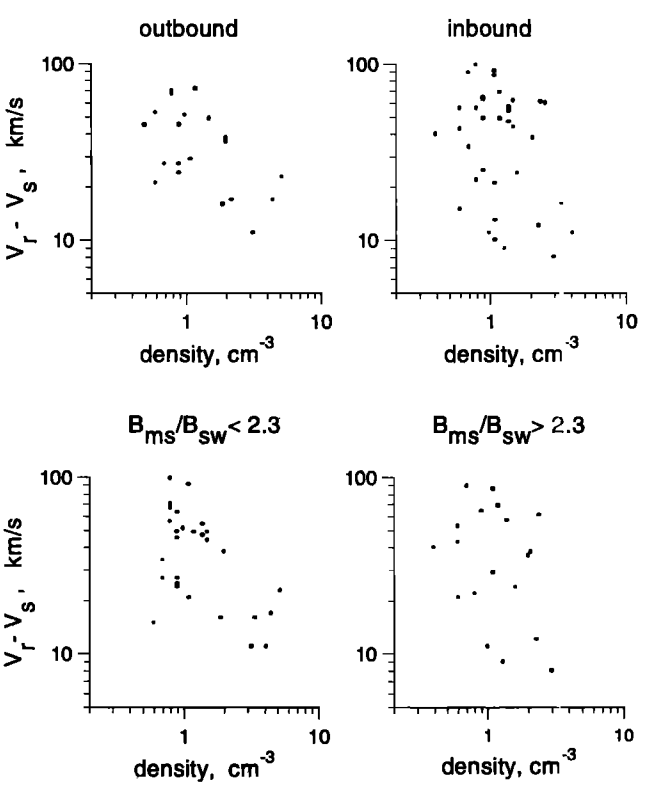

Figure 4. Velocity decrease V_r - V_s versus reference solar wind density for the outbound crossings (correlation coefficient c = 0.54), for the inbound crossing (c = 0.31), for bow shock crossings with $B_{ms}/B_{sw} < 2.3$ (c = 0.54), and with $B_{ms}/B_{sw} > 2.3$ (c = 0.31).

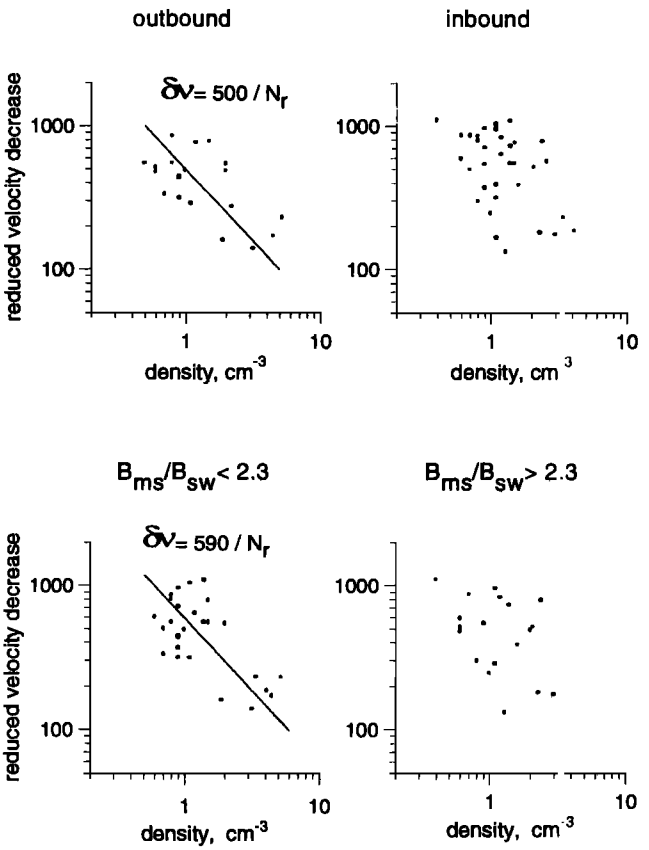

Figure 5. Reduced velocity decrease δv with n_1/n_o= 1/3 in (4) versus reference solar wind density for the same groups of bow shock crossings as in Figure 4. Solid lines represent the best fits. Calculated correlation coefficients are as follows c=0.61 for the outbound crossings, c=0.46 for the inbound crossings, c=0.65 for the crossings with $B_{ms}/B_{sw} < 2.3$, and c=0.4 for the crossings with $B_{ms}/B_{sw} > 2.3$.

where $f_s = f(r_s, \varphi_s, n_1/n_o, \gamma)$, $f_r = f(r_r, \varphi_r, n_1/n_o, \gamma)$, $g_r = g(r_r, \varphi_r, n_1/n_o, \gamma)$, the subscript s refers to the point just upstream of the bow shock, and the subscript r refers to the point ~50 min upstream of the bow shock. In a linear approximation the following expression can be obtained:

$$\delta v \equiv \frac{V_r - V_s}{f_s - f_r}\frac{\tau_i}{M_i r_o}\left(1 - \frac{V_r - V_s}{f_s - f_r}\cdot\frac{g_r}{V_r}\right) = \frac{n_o}{N_r}, \qquad (4)$$

where the reduced velocity decrease δv is inversely proportional to the observed reference solar wind density.

Figure 5 shows the reduced velocity decrease taking n_1/n_o = 1/3 versus solar wind density for the same four groups of bow shock crossings as in Figure 4. Particularly in the case of bow shock crossings with small magnetic field jump $B_{ms}/B_{sw} < 2.3$, the correlation becomes better than in Figure 4. Taking into account only the effect of the hot oxygen corona, least square fitting in the case of n_1/n_o =1/3 provides n_o = 500±100 cm^{-3} for the outbound crossings and n_o = 590 ± 100 cm^{-3} for the crossings with the ratio $B_{ms}/B_{sw} < 2.3$. In case of n_1/n_o =1, as suggested by *Verigin et al.* [1991], the following parameters are obtained: n_o = 340 ± 80 cm^{-3} for the outbound crossings and n_o = 410 ± 80 cm^{-3} for the crossings with $B_{ms}/B_{sw} < 2.3$.

Only the crossings of the shock supposed to be quasi-parallel have been considered for the estimation of the density in the planetary corona in the meanwhile. However, the loading of the solar wind flow by planetary ions is assumed to be dawn-dusk

symmetric, and that is why it is worthwhile to consider the quasi-perpendicular shock crossings too. Another reason to do this is that the region upstream from the foot of the quasi-perpendicular shock is inaccessible to particles originating at the shock, and thus the influence of foreshock ions on the solar wind flow could be excluded.

Figure 6 presents the reduced velocity decrease calculated with the new values of V_s and f_s in (4) versus reference solar wind density for the same four groups of bow shock crossings as in Figures 4 and 5. These new V_s and f_s values were taken 5 min upstream of the bow shock crossing in order to minimize the role of specularly reflected protons which are mostly effective in the shock foot (see Figure 3). Now in all cases the correlations are better than in Figure 5, and the parameters n_o are approximately equal for all groups of crossings. New estimations of the parameter n_o are $n_o \approx 370 \pm 50$ cm^{-3} for $n_1/n_o = 1/3$ and $n_o \approx 250 \pm 40$ cm^{-3} for $n_1/n_o = 1$ for the coronal density profile (2).

Discussion

The TAUS instrument measurements onboard the Phobos 2 spacecraft show that the solar wind flow deceleration upstream of the Martian bow shock is a common feature of the solar wind - Mars interaction. It was observed in all three subsolar bow shock crossings where TAUS data were available [*Verigin et al.*, 1991] and in most bow shock crossings (both inbound and outbound) near the terminator plane (Figure 1). The relative solar wind velocity decrease is 1.5-2 times larger and more abrupt upstream of the dusk side (inbound) bow shock crossings than upstream of the dawn side (outbound) crossings, where velocity decreases rather gradually (Figure 3). This difference is apparently a consequence of the fact that quasi-perpendicular bow shock crossings are more frequent on the dusk side and quasi-parallel shock crossings are more frequent on the dawn side.

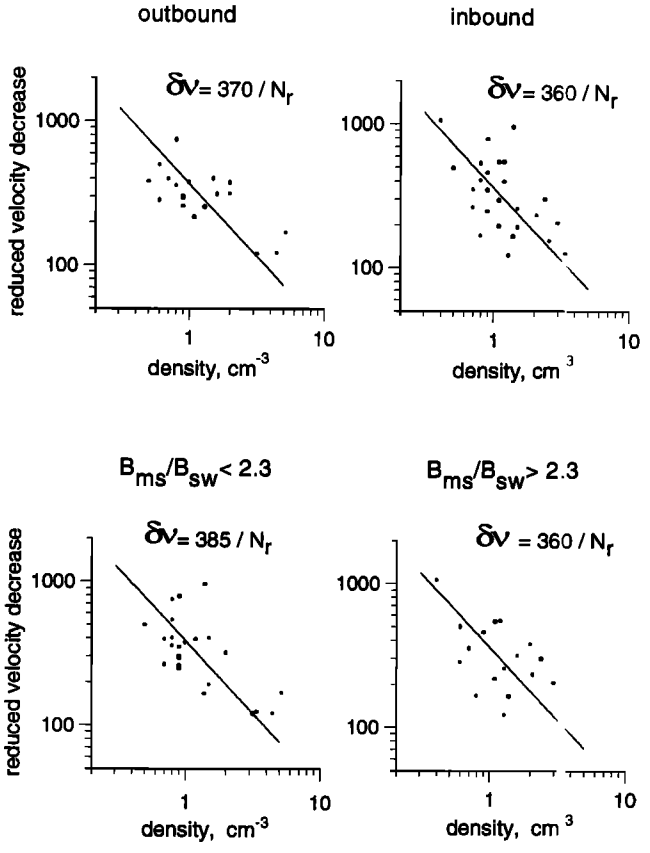

Figure 6. Reduced velocity decrease δv calculated by (4) with $n_1/n_o = 1/3$ and V_s, f_s taken 5 min upstream of the shock crossing versus reference solar wind density for the outbound crossings (correlation coefficient c = 0.7), for the inbound crossing (c = 0.56), for bow shock crossings with $B_{ms}/B_{sw} < 2.3$ (c = 0.66), and for those with $B_{ms}/B_{sw} > 2.3$ (c = 0.47).

As it was mentioned in the introduction, there are two possible reasons for the deceleration of the solar wind upstream of the Martian bow shock: (1) mass loading of the solar wind by ions originating from the planetary corona, and (2) protons reflected from the bow shock.

The analysis of the solar wind deceleration upstream of the Martian terminator bow shock revealed that for the outbound bow shock crossings and for the crossings with rather small magnetic field jump at the shock the value of velocity decrease is roughly inversely proportional to the density of the solar wind. This fact suggests that the Martian oxygen/hydrogen corona might influence the observed deceleration effect in case of these crossings.

The number of specularly reflected protons which can also cause solar wind velocity decrease depends on different solar wind parameters: the angle ϑ_{BN}, upstream Mach numbers, plasma parameter β, ratio of specific heats, etc. [*Wilkinson and Schwartz*, 1990]. Among these parameters only Alfvenic Mach number M_A and β depend on the solar wind density. Since the number of reflected ions relative to the number of incident ions is likely to increase with M_A and β [*Wilkinson and Schwartz*, 1990], the solar wind deceleration should increase with increasing plasma density, contrary to the case of mass loading by planetary ions.

As was already mentioned, the solar wind deceleration upstream of the Martian quasi-parallel bow shock could be caused by the so-called diffuse ions backstreaming from the shock [*Bame et al.*, 1980; *Bonifazi et al.*, 1980]. However, it seems impossible to explain the experimental results obtained as the effect of only these ions. Indeed, the value of velocity decrease upstream of the Martian bow shock (20-30 km s^{-1}, Figure 4, left plots) is higher on average than that observed near the Earth (7-10 km s^{-1}, changes in speed of 25-40 km s^{-1} were only occasionally recorded [*Bame et al.*, 1980]). Furthermore, the density of the diffuse backstreaming ions is proportional to the density of the incident solar wind [*Tratner et al.*, 1994], and hence their deceleration effect would not depend on the solar wind density in contradiction to the relation revealed here between the velocity decrease and upstream solar wind density in case of quasi-parallel bow shock near Mars.

However, the direct relationship between the velocity decrease and the density has not been tested with the data obtained near the Earth or any other planet. Thus it should be noted that the strength of the conclusions in this study depends somewhat on establishing such a relationship in the absence of planetary corona, and the present estimations of the planetary corona density should be considered as an upper limit now.

Assuming that the solar wind deceleration upstream of the foot of the bow shock is mainly caused by the presence of the hot oxygen corona of Mars and using the same model of the oxygen corona [*Ip*, 1988, 1990] which was used by *Verigin et al.* [1991], (4) permits us to estimate the parameter n_o of the density profile (2) of hot oxygen $n_o(r)$ in the Martian corona as $n_o \approx 370 \pm 50$ cm^{-3} when $n_1/n_o = 1/3$, corresponding to the model profile of *Ip* [1988,

1990], and $n_o \approx 250\pm40$ cm^{-3} when $n_i/n_o = 1$. The approximate equality of n_o values for all groups of crossings (Figure 6) suggests that the solar wind slowing associated with the pickup process is more or less dawn-dusk symmetric. Besides, close coincidence of the fitting parameters referred to the inbound and outbound cases can also be considered as an argument of relatively small contribution of foreshock ions to the solar wind deceleration.

The smaller value of n_o obtained for the outbound crossings and the crossings with small magnetic field jump (Figure 6) when the solar wind deceleration upstream of the shock foot was considered, in comparison to the first estimation (Figure 5) is likely to be a consequence of the fact that sometimes the quasi-perpendicular bow shock was crossed in these cases, and specularly reflected protons in the foot of the shock affect the first estimation of n_o.

Figure 7 shows the height profiles of the oxygen corona density when n_o = 370 cm^{-3} for n_i/n_o = 3 (thin solid curve) and n_o = 250 cm^{-3} for n_i/n_o = 1 (dashed curve). These profiles are more reliable near the heights of Phobos 2 circular orbit, and they intersect each other at ~ 6800 km (open circle). Also in figure 7, two additional profiles are shown obtained by *Verigin et al.*, [1991] on the basis of the data received from the elliptical orbits (dotted curve shows the profile with parameters n_o = 500 cm^{-3} and n_i/n_o = 1/3, while in the case of the dashed-dotted curve n_o = 200 cm^{-3} and n_i/n_o = 1). These profiles intersect at ~ 1400 km (open circle) and are obviously more reliable near the height of the subsolar bow shock. From Figure 7 it is seen that on low altitudes the profiles determined from the observations upstream of the subsolar bow shock lie in between the profiles obtained from the data near the terminator plane, while on higher altitudes there is an opposite situation. All the profiles define a "confidence band" for an "optimal" coronal density profile, which passes through the marked points of intersection and could be described by relation (2) with parameters n_o = 310 cm^{-3} and n_i/n_o = 0.6 (thick solid curve in Figure 7). This optimal profile is in reasonable agreement with the observations of solar wind deceleration upstream of the subsolar bow shock and also with the revealed correlation between the reduced velocity decrease and the solar wind density upstream of the bow shock near the terminator plane.

Generally speaking, the profile obtained describes not only the oxygen corona but also that $n(r)$ depends on both oxygen and hydrogen corona densities. The velocity decrease upstream of the bow shock, resulting from the Martian corona, is proportional to

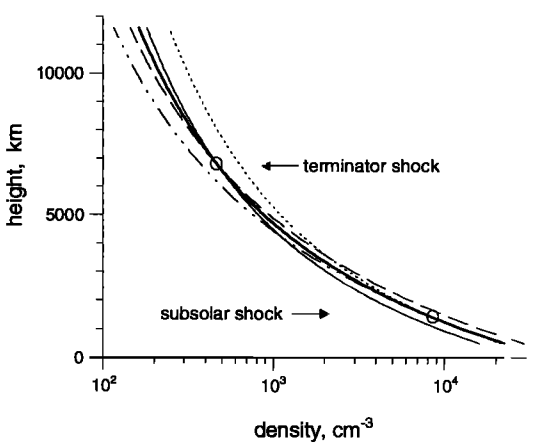

Figure 7. Height profiles of the oxygen corona density.

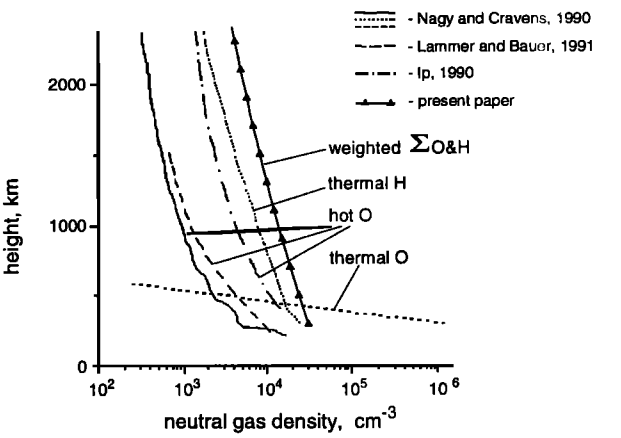

Figure 8. Comparison of the obtained density profile in the neutral corona of Mars with height profiles of existing density distribution models of the oxygen and hydrogen corona of Mars.

the mass of loading ions and to the density in the corona, while it is inversely proportional to the time of ionization (1). If the density profile in the hydrogen corona $n_H(r)$ can be approximately described by a relation similar to (2), then the profile obtained should be attributed to

$$n(r) = n_O(r) + n_H(r)\frac{M_H}{M_O}\frac{\tau_O}{\tau_H} \approx 310\left(\frac{r_o}{r}\right)^2\left[1+\frac{3}{5}\left(\frac{r_o}{r}\right)^3\right], \quad (5)$$

where M_O and τ_O and M_H and τ_H are the masses and the ionization times of oxygen and hydrogen, respectively.

The above described profile is plotted by the solid curve with triangles in Figure 8 together with existing density distribution models of the Martian oxygen and those of hydrogen corona. If this profile is fully attributed to the hot oxygen corona, the corresponding oxygen densities would be ~ 4-5 times higher than those of the hot oxygen models of *Ip* [1988, 1990], and the discrepancy with other models [*Nagy and Cravens*, 1988, 1990; *Lammer and Bauer*, 1991] is even more significant.

Let us consider how the above estimations can change, taking into account the effect of the hydrogen corona of Mars. Picked-up protons originating from the hydrogen corona of Mars were observed in the upstream solar wind by the ASPERA experiment onboard Phobos 2 [*Barabash et al.*, 1991]. Thermal hydrogen densities in the Martian corona were deduced on the basis of Lyman alpha observations onboard Mariner 6,7, and 9 and Mars 2 and 3 [*Anderson*, 1974; *Dostovalov and Chuvahin*, 1973] in the period near the solar minimum, but the density of hot oxygen has never been measured near Mars. During solar minimum conditions, thermal hydrogen densities can be 10 times larger than hot oxygen densities [*Nagy and Cravens*, 1988, 1990; *Lammer and Bauer*, 1991], as shown in Figure 7. It may be supposed that the same relationship is valid for solar maximum conditions which are appropriate for Phobos 2 observations.

The total time of ionization can be estimated by the expression

$$\frac{1}{\tau_i} = \frac{1}{\tau_{ph}} + \frac{1}{\tau_{ce}} + \frac{1}{\tau_{ei}}, \quad (6)$$

where τ_{ph} is the time of photoionization, τ_{ce} is the time of charge exchange, and τ_{ei} is the time of electron impact ionization. Near the orbit of Mars, $\tau_O \approx 2\times10^6$ s ($\tau_{ph} \approx 1.4\times10^6$ s, $\tau_{ce} \approx 4\times10^6$ s, and $\tau_{ei} \approx 2\times10^7$ s at 1 AU) for atomic oxygen, and $\tau_H \approx 3\times10^6$ s ($\tau_{ph} \approx 10^7$ s, $\tau_{ce} \approx 1.7\times10^6$ s, and $\tau_{ei} \approx 5\times10^7$ s at 1 AU) for

atomic hydrogen [*Cravens et al.*, 1987]. Taking into account the difference in masses, the hydrogen corona of Mars can contribute up to 30% of the effect of the hot oxygen corona in the deceleration of the solar wind upstream of the bow shock. Even if this contribution of the hydrogen corona is taken into account, hot oxygen densities are still ~ 3 times higher than the values in the most intense model of *Ip* [1988,1990].

In the above consideration only the contribution of the oxygen and hydrogen corona to the solar wind preshock deceleration was discussed. *Barabash and Norberg* [1994] concluded that the helium corona may also play a role in the solar wind mass loading process near Mars. However, even according to the "maximum" engineering model of *Moroz et al.* [1991] (exponentially extrapolated to the altitudes higher than 450 km, cf. *Barabash and Norberg* [1994]), the density of hydrogen exceeds the density of helium in the Martian corona at altitudes $\geq$ 1200 km. All the Martian bow shock crossings by Phobos 2 occur at higher altitudes (~ 1500 km for the subsolar crossings and ~ 6300 km for the terminator crossings). Since the ionization time of helium [Barabash and Norberg, 1994] is about an order of magnitude longer than τ_H, the contribution of the helium corona to solar wind deceleration can be neglected.

Conclusions

Solar wind plasma and magnetic field data obtained near the Martian terminator bow shock onboard the Phobos 2 spacecraft in its circular orbits have been analyzed. It is revealed that on average the solar wind stream is slowing down upstream of the bow shock. The relative solar wind velocity decrease is about 7% of the reference solar wind velocity upstream of the inbound (dusk side) bow shock crossings and ~ 4% upstream of the outbound (dawn side) crossings, the deceleration being more abrupt on the dusk side. A similar difference is observed if one separates the bow shock crossings according to the jump in magnetic field magnitude. This is apparently a consequence of observing mostly quasi-perpendicular bow shocks on the dusk side while mostly quasi-parallel shocks on the dawn side.

For the outbound (quasi-parallel) bow shock crossings a nearly inverse correlation is revealed between the values of velocity decrease and the undisturbed solar wind density, while for the inbound crossings this correlation is observed only for the velocity decrease upstream of the shock foot. This fact permits us to distinguish between the two possible reasons causing solar wind deceleration: (1) mass loading of the solar wind flow by planetary ions originating from the corona of Mars, and (2) solar wind protons reflected from the bow shock. Upstream of the bow shock foot the solar wind deceleration turned to be dawn-dusk symmetric.

The revealed relation between the reduced velocity decrease upstream of the bow shock foot and the solar wind density permits us to obtain density profiles for the hot oxygen/hydrogen corona which are most reliable at the height of ~ 6800 km. The optimal corona density profile (5) was also deduced in agreement with the observations of solar wind deceleration upstream of the subsolar bow shock [*Verigin et al.*, 1991]. However, the density values of the hot oxygen corona of Mars are ~ 3 times higher according to this profile than those predicted by the "extreme" corona model [*Ip*, 1988,1990], even when the possible contribution of the hydrogen corona to the solar wind deceleration effect is taken into account. These estimations of the coronal density are only valid when the loading by planetary ions is the main cause of solar wind deceleration, and thus they should be considered as an upper limit now.

Acknowledgments. The research described in this publication was made possible in part by grants MQU000/300 from ISF, 94-982 from INTAS, and 95-02-04223 from RFFE, by grant OTKA T 015866 of the Hungarian Science Fund, and by the Hungarian-Russian Intergovernmental S&T Cooperation Programme (project 28).

The Editor thanks T.G.Onsager and another referee for their assistance in evaluating the paper.

References

Anderson, D.E., Mariner 6,7, and 9 ultraviolet spectrometer experiment: Analysis of hydrogen Lyman alpha data, *J. Geophys. Res.*, *79*, 1513-1518, 1974.

Aydogar, Ö., K. Schwingenschuh, G. Schelch, H. Arnold, G. Berghofer, and W. Riedler, The Phobos fluxgate magnetometer (MAGMA) instrument description, *Rep. IWF-8904*, 28 pp., Space Research Institute Austrian Academy of Sciences, Graz, Austria, 1989.

Bame, S.J., J.R. Asbridge, W.C. Feldman, J.T. Gosling, G. Paschmann, and N. Sckopke, Deceleration of the solar wind upstream from the Earth's bow shock and the origin of diffuse upstream ions, *J. Geophys. Res.*, *85*, 2981-2990, 1980.

Barabash, S., and R. Lundin, Reflected ions near Mars: Phobos 2 observations, *Geophys. Res. Lett.*, *20*, 787-790, 1993.

Barabash, S., and O. Norberg, Indirect detection of the Martian helium corona, *Geophys. Res. Lett.*, *21*, 1547-1550, 1994.

Barabash, S., E. Dubinin, N. Pissarenko, R. Lundin, and C.T. Russell, Picked-up protons near Mars: Phobos observations, *Geophys. Res. Lett.*, *18*, 1805-1808, 1991.

Bonifazi, C., G. Moreno, A.J. Lazarus, and J.D. Sullivan, Deceleration of the solar wind in the Earth's foreshock region: ISEE 2 and IMP 8 observations, *J. Geophys. Res.*, *85*, 6031-6038, 1980.

Cravens, T.E., J.U. Kozyra, A.F. Nagy, T.I. Gombosi, and M. Kurtz, Electron impact ionization in the vicinity of comets, *J. Geophys. Res.*, *92*, 7341-7353, 1987.

Dostovalov, S.B., and S.D. Chuvahin, On the distribution of neutral hydrogen in the upper atmosphere of Mars (in Russian), *Kosm. Issled.*, *11*, 767-773, 1973.

Dubinin, E., D. Obod, A. Pedersen, and R. Grard, Mass loading asymmetry in the upstream region near Mars, *Geophys. Res. Lett.*, *21*, 2769-2772, 1994.

Goodrich, C.C., Numerical simulations of quasi-perpendicular collisionless shocks, in *Collisionless Shocks in the Heliosphere: Reviews of Current Research, Geophys. Monogr. Ser.*, vol. 35, edited by B.T. Tsurutani and R.G. Stone, pp.153-168, AGU, Washington, D.C., 1985.

Gosling, J.T. and A.E. Robson, Ion reflection, gyration and dissipation at supercritical shocks, in *Collisionless Shocks in the Heliosphere: Reviews of Current Research, Geophys. Monogr. Ser.*, vol.35, edited by B T. Tsurutani and R.G. Stone, pp.141-152, AGU, Washington, D.C., 1985.

Gosling, J.T., M.F.Thomsen, S.J.Bame, W.C.Feldman, G.Paschmann, and N.Sckopke, Evidence for specularly reflected ions upstream from the quasi-parallel bow shock, *Geophys. Res. Lett.*, *9*, 1333-1336, 1982.

Ip, W.-H., On a hot oxygen corona of Mars, *Icarus*, *76*, 135-145, 1988.

Ip, W.-H., The fast atomic corona extension of Mars, *Geophys. Res. Lett.*,**17**, 2289-2292, 1990.

Lammer, H., and S.J. Bauer, Nonthermal atmospheric escape from Mars and Titan, *J. Geophys. Res.*, *96*, 1819-1825, 1991.

Moroz, V.I., V.V. Kerzhanovich, and V.A. Krasnopolsky, An engineering model of the atmosphere of Mars for the Mars-94 project (MA-90), *Cosmic Res.*, Engl. Transl., *29*, 1-79, 1991.

Nagy, A.F., and T.E. Cravens, Hot oxygen atoms in the upper atmospheres of Venus and Mars, *Geophys. Res. Lett.*, *15*, 433-435, 1988.

Nagy, A.F., and T.E.Cravens, Hot hydrogen and oxygen atoms in the upper atmospheres of Venus and Mars, *Ann. Geophys.*, *8*, 251-256, 1990.

Neugebauer, M., Initial deceleration of solar wind positive ions in the Earth's bow shock, *J. Geophys. Res.*, *75*, 717-733, 1970.

Onsager, T.G., and M.F. Thomsen, The Earth's foreshock, bow shock, and magnetosheath, *U.S. Natl. Rep. Int. Union Geod. Geophys.* 1987-1990, *Rev. Geophys.*, *29*, 998-1007, 1991.

Rosenbauer, H., et al., The study of three dimensional distribution functions of the main solar wind ions - protons and alpha-particles - in the Pho-

bos mission: TAUS experiment (MPK instrumentation), in *The Instrumentation and Methods in Space Research* (in Russian), edited by V.M.Balebanov, pp.30-43, Nauka, Moscow, 1989a.

Rosenbauer H., et al., Ions of Martian origin and plasma sheet in the Martian magnetosphere: initial results of the TAUS experiment, *Nature*, *341*(6243), 612-614, 1989b.

Sckopke, N., G. Paschmann, S.J. Bame, J.T. Gosling, and C.T. Russell, Evolution of ion distributions across the nearly perpendicular bow shock: Specularly and nonspecularly reflected-gyrating ions, *J. Geophys. Res.*, *88*, 6121-6136, 1983.

Slavin, J.A., K. Schwingenschuh, W. Riedler, and Y. Yeroshenko, The solar wind interaction with Mars: Mariner 4, Mars 2, Mars 3, Mars 5, and Phobos 2 observations of bow shock position and shape, *J. Geophys. Res.*, *96*, 11,235-11,241, 1991.

Tatrallyay, M., C.T. Russell, J.G. Luhmann, A. Barnes, and J.D. Mihalov, On the proper Mach number and ratio of specific heats for modeling the Venus bow shock, *J. Geophys. Res.*, *89*, 7381-7392, 1984.

Tratner, K.J., E. Möbius, M. Scholer, B. Klecker, M. Hilchenbach, and H. Luhr, Statistical analysis of diffuse ion events upstream of the Earth's bow shock, *J. Geophys. Res.*, *99*, 13,389-13,400, 1994.

Verigin, M.I., K.I. Gringauz, G.A. Kotova, N.M. Shutte, H. Rosenbauer, S. Livi, A.K. Richter, W. Riedler, K. Schwingenschuh, and K. Szegö, On the problem of the Martian atmosphere dissipation: Phobos 2 TAUS spectrometer results, *J. Geophys. Res.*, *96*, 19,315-19,320, 1991.

Wilkinson, W.P., and S.J. Schwartz, Parametric dependence of the density of specularly reflected ions at quasi-perpendicular collisionless shocks, *Planet. Space Sci.*, *38*, 419-435, 1990.

Zhang, T.-L., K. Schwingenschuh, H. Lichtenegger, W. Riedler, C.T. Russell, and J.G. Luhmann, Interplanetary magnetic field control of the Mars bow shock: Evidence for Venuslike interaction, *J. Geophys. Res.*, *96*, 11,265-11,269, 1991.

G. Kotova, A. Remizov, N. Shutte, and M. Verigin, Space Research Institute, Profsoyuznaya 84/32, Moscow 117810, Russia. (e-mail: gkotova@vmcom.lz.space.ru; aremizov@vmcom.lz.space.ru; nshutte@vmcom.lz.space.ru; mverigin@esoc1.iki.rssi.ru)

J. Lemaire, Belgisch Instituut voor Ruimte-Aeronomie, Ringlaan 3, B-1180, Brussels, Belgium. (e-mail: jl@plasma.oma.be)

S. Livi and H. Rosenbauer, Max-Planck-Institut für Aeronomie, D-37191 Katlenburg-Lindau, Germany. (e-mail: slivi@linax1.mpae.gwdg.de; rosenbauer@linax1.mpae.gwdg.de)

K Schwingenschuh and T.-L. Zhang, Space Research Institute, Inffeldgasse 12, 8010 Graz, Austria. (e-mail: schwingen@fiwf01.tu-graz.ac.at; zhang@fiwf02.tu-graz.ac.at)

J Slavin, NASA Goddard Space Flight Center, Code 696, Greenbelt MD 20771. (e-mail: slavin@lepjas.gsfc.nasa.gov)

K. Szego and M. Tatrallyay, KFKI Research Institute for Particle and Nuclear Physics, 1525 Budapest P.O. Box 49, Hungary. (e-mail: szego@rmki.kfki.hu; mariella@rmki.kfki.hu)

(Received June 12, 1995; revised May 14, 1996;
accepted May 14, 1996.)